View metadata, citation and similar papers at core.ac.uk

brought to you by CORE

provided by Queensland University of Technology ePrints Archive

COVER SHEET

This is the author version of article published as:

Momot, Konstantin I. and Kuchel, Philip W. (2004) Convection-compensating PGSE experiment incorporating excitation-sculpting water suppression (CONVEX). Journal of Magnetic Resonance 169(1):pp. 92-101.

Copyright 2004 Elsevier

Accessed from http://eprints.qut.edu.au

Convection-compensating PGSE experiment incorporating excitation-sculpting water suppression (CONVEX)

Konstantin I. Momot and Philip W. Kuchel

School of Molecular and Microbial Biosciences, University of Sydney,
Sydney, NSW 2006, Australia

Revised version 26/03/2004 7:59 AM

Address for correspondence: Konstantin Momot
School of Molecular and Microbial Biosciences
Building G08
University of Sydney
NSW 2006
Australia

E-mail address: konstantin@usyd.edu.au

Running title: Convection Compensation with Water Suppression

Keywords: excitation sculpting solvent suppression;
convection-compensating PGSE;
diffusion and flow measurements by NMR;
Stejskal–Tanner plots

Abbreviations: DMMP, dimethyl methylphosphonate;
LSF, least-squares fit;
MQ(F), multiple-quantum (filtered);
MW, molecular weight;
PBS, phosphate-buffered saline;
PFG, pulsed field gradient;
PGSE; pulsed-field gradient spin echo;
SE, spin echo.

Abstract

We present a new diffusion experiment which provides simultaneous suppression of an on-resonance solvent peak and compensation for convection. The experiment, which we name CONVEX, exploits similarities between two functionally different pulse sequences to enable the same sequence to be used simultaneously for two different purposes. The CONVEX pulse sequence combines a double-echo PGSE with double excitation-sculpting water suppression, using unequal gradient pulse-pair amplitudes (g_1 and g_2) and unequal diffusion intervals (Δ_1 and Δ_2). Convection compensation is achieved by setting $g_1 : g_2 = \Delta_2 : \Delta_1$. The new experiment provides the spectral quality, flat baseline, and water-suppression power characteristic of excitation-sculpting experiments, combined with excellent compensation for convection. The resulting Stejskal–Tanner plots are linear over a greater range of signal attenuation than in the absence of water suppression. Possible applications include protein NMR; NMR of cellular or colloidal systems; and monitoring of technological processes.

Introduction

Our aim is to present a novel diffusion-measurement experiment which provides simultaneous suppression of an on-resonance solvent peak and compensation for convection. The experiment, which we named CONVEX for "CONVection compensation/EXcitation sculpting", exploits similarities between two functionally different pulse sequences to enable the same sequence to be used simultaneously for two different purposes. This approach is similar to the recently proposed PGSE-Watergate experiment [1]; however, our experiment differs from PGSE-Watergate both by design and functionally.

Solvent suppression is often a pre-requisite for obtaining high-quality ^{1}H NMR spectra from samples containing large quantities of protonated solvent. This may be the case when the amount of solute is prohibitively small for reconstitution in deuterated solvent [2], or when the sample is produced biologically and solvent replacement is not possible [3,4]. Some of the general approaches exploited for the purpose of suppressing the solvent peak are: (1) multiple-quantum, diffusion or relaxation filtering; (2) relaxation enhancement or saturation of the solvent peak; (3) selective echo refocusing; or (4) selective excitation using composite or frequency-selective pulses [5,6]. Solvent suppression in the proposed CONVEX experiment is based on excitation sculpting [5], which provides a powerful means of eliminating dynamic-range problems associated with a large solvent peak.

Thermal convection can interfere with NMR diffusion measurements in solution, especially at non-ambient temperatures and/or in low-viscosity liquids [7]. A number of well-known strategies are available to deal with this problem, including: (1) increasing the aspect ratio (length:diameter) of the sample [8,9]; (2) minimization of temperature inversion inside the sample through improved design of temperature control; (3) using transverse (x, y) instead of longitudinal (z) pulsed field gradients; and (4) using a convection-compensating pulsed-gradient sequence [7,10,11]. The last approach is probably the most versatile of the four, because the convection compensation in it is achieved through a clever design of the experimental pulse sequence, and no special hardware requirements or sample geometry limitations are imposed, beyond those already inherent in PFG NMR diffusion measurements.

Background

Next, we briefly review PFG NMR measurements of diffusion and flow, with the aim of isolating the formal requirements that enable convection compensation [12,13]. We also review excitation-sculpting water suppression, and examine why the quality of spectra it produces is superior to most of the earlier methods.

Convection compensation in diffusion measurements

In the presence of both random diffusion and uniform steady-state plug flow [14], the signal S detected in a PFG NMR experiment can be expressed in a general form as [10,15]

$$S(q) = S(0)\, e^{-D\gamma^2 \int_0^{t_s} q^2(t)\,dt} \quad e^{i\gamma \mathbf{v} \cdot \int_0^{t_s} \mathbf{q}(t)\,dt} \tag{1}$$

where D is the diffusion coefficient of the measured species; γ, the magnetogyric ratio; $\mathbf{v}$, the velocity of the flow; and t_s, the duration of the pulse sequence [from the first radiofrequency (RF) excitation pulse to the beginning of signal acquisition]. The spatial wave vector $\mathbf{q}$ specifies the tightness of the magnetization helix wound by the field gradient pulses:

$$\mathbf{q}(t) = \int_0^t \gamma\, p(t')\, \mathbf{g}(t')\, dt' \tag{2}$$

where g is the field gradient amplitude and p is the selected coherence order [16].

Equation (1) can be extended to describe the effects of convective flow. If the convection is both slow and steady-state, then $\mathbf{v}$ within a given volume element remains approximately constant throughout t_s. The total signal then behaves as

$$S(q) \approx S(0)\, e^{-D\gamma^2 \int_0^{t_s} q^2(t)\,dt} \times \int_V e^{i\gamma \mathbf{v}(\mathbf{r}) \cdot \int_0^{t_s} \mathbf{q}(t)\,dt}\, d\mathbf{r} \tag{3}$$

where the second exponential is integrated over the sample volume. Because the average $\mathbf{v}$ in a closed sample is zero, convection effectively results in additional signal attenuation, thus increasing the value of the apparent diffusion coefficient.

On the other hand, if the pulse sequence is designed so as to satisfy the condition,

$$\int_0^{t_s} \mathbf{q}(t)\, dt = 0 \tag{4}$$

and assuming that the zero-acceleration and steady-state flow approximations hold, then the second exponential in Eq. (3) is identically equal to 1, and the detected signal is insensitive to flow. Of course, the normal spin-echo refocusing condition,

$$\mathbf{q}(t_s) = 0 \tag{5}$$

also applies. Equations (4) and (5) constitute the criteria that define the family of convection-compensating pulse sequences [10].

The CONVEX experiment is based on a diffusion-compensating PGSE sequence by Sørland et al [11], which is shown in Fig. 1A. This sequence consists of two spin-echo blocks of the form $G - \pi - G$, where G is a gradient pulse, π is a refocusing RF π-pulse, and all four gradient pulses have the same amplitude and direction. The diffusion-sensitive grating is wound by the first gradient pulse and refocused by the second one. The third and fourth gradient pulses repeat this operation, but the wound grating has the opposite-sign wave vector **q**, thus making the overall time integral of **q** equal to zero. In the rectangular-gradient pulse approximation, the amplitude of the signal depends on the gradient strength g as [11]

$$S(g) = S(0)e^{-2D\gamma^2 g^2 \delta^2 (\Delta - \delta/3)} \tag{6}$$

where the meaning of δ and Δ is shown in Fig. 1A. The slope of the respective ideal Stejskal–Tanner plot is therefore twice that of the basic PGSE experiment.

Excitation-sculpting water suppression

Excitation sculpting is a class of sequences of the type $[G_i - S - G_i]^n$, where G_i are gradient pulses and S is a potentially arbitrary combination of hard and soft RF pulses and delays. Its use for solvent suppression is based on the following idea [5]. Suppose S is a selective-inversion operator which inverts the magnetization of off-resonance solute but not on-resonance solvent. The block $[G_1 - S - G_1]$ then provides solvent suppression by refocusing off-resonance, but not on-resonance, peaks. Inevitably, the suppression profile is imperfect, and a residual solvent signal $P << 1$ is present after a single application. Applying this sequence twice with the same S but $G_2 \neq G_1$ leaves a smaller residual solvent signal P^2. Even more importantly, the corresponding rotation operator is diagonal after the double application even if it is not after a single one. This means the phase of both solute and solvent magnetization is preserved; in practical terms this yields pure-phase spectra without baseline distortions.

Our immediate focus is a pulse sequence with S = (soft-π_{-x} – hard-π_x). Double application of this selective-refocusing operator, shown in Fig. 1B, has been shown to produce almost perfect water suppression devoid of spectral baseline or phase distortions. In the next section, we show how double-echo excitation-sculpting can be incorporated into the convection-compensating PGSE diffusion experiment of Fig. 1A.

The CONVEX experiment

The experiments in Figs. 1A and 1B are obviously similar and rely on the same spin-echoes forming at the end of each bracketed time interval. However, when attempting to combine them, we face the apparently contradictory requirements with respect to the amplitude of the two gradient pulse pairs (g_1 and g_2). Efficient solvent suppression calls for $g_1 \neq g_2$, and preferably their being non-multiples of each other. On the other hand, convection compensation apparently requires $g_1 = g_2$, which would significantly decrease the efficiency of solvent suppression because of signal leakage [17]. This contradiction is resolved by noting that the durations of the two diffusion intervals can be made unequal, i.e., $\Delta_1 \neq \Delta_2$. Because only the integrals of $|\mathbf{q}|$ in the two diffusion intervals, rather than the respective maximum values, have to be equal for convection compensation to be achieved, the amplitudes of the two pairs of gradients can be made to relate inversely to diffusion interval durations, viz.,

$$g_2 : g_1 \; = \; \Delta_1 : \Delta_2 \; = C \tag{7}$$

Equation (7) satisfies each requirement: solvent suppression (unequal gradient pair amplitudes filter out signal leakage), convection compensation [Eq. (4)], and spin-echo refocusing [Eq. (5)]. The corresponding pulse sequence (CONVEX) is shown in Fig. 2A. The evolution of the magnetization grating wave vector, **q**, is shown in Fig. 2B; the areas of the two shaded trapezoids are equal if Eq. (7) is satisfied. To minimize the effect of possible eddy currents, we used $C < 1$ [5], i.e., the second diffusion interval was longer and the second pair of gradient pulses had a lower amplitude.

Applying Eqs. (1) and (2) to the CONVEX pulse sequence yields signal attenuation as a function of the experimental parameters. In the rectangular-gradient pulse approximation, the amplitude of the signal is given by

$$S(g) = S(0) e^{-D\gamma^2 g_1^2 \delta^2 \left[\Delta_1 (1+C) - \frac{\delta (1+C^2)}{3} \right]} \tag{8}$$

The resulting plot of ln S vs g_1^2 is linear, as the terms in the square brackets are constant. Other gradient pulse shapes can also be used. For trapezoidal pulses with ramp time τ and effective duration δ, the signal amplitude is given by

$$S(g) = S(0) e^{-D\gamma^2 g_1^2 \left[\Delta_1 \delta^2 (1+C) - \frac{\delta^3 (1+C^2)}{3} - \frac{\delta \tau^2 (1+C^2)}{6} + \frac{\tau^3 (1+C^2)}{30} \right]} \tag{9}$$

which simplifies to Eq. (8) when $\tau \rightarrow 0$. For sine gradient pulses, the integration of Eq. (1) yields

$$S(g) = S(0)e^{-\frac{D\gamma^2 g_1^2 \delta^2}{\pi^2}\left[4\Delta_1(1+C) - \delta(1+C^2)\right]} \quad (10)$$

where δ is the duration of the half period-long sinusoidal pulse.

Materials and methods

Sample preparation

Reagents were purchased from the following sources: dimethyl methylphosphonate (DMMP, min. 97%), from Fluka Chemie AG (Buchs, Switzerland); carbon tetrachloride (spectroscopic grade), from AJAX Chemicals (Auburn, NSW, Australia); lysozyme, from Sigma (St. Louis, MO). All chemicals were used as received. Water was obtained from a Milli-Q reverse-osmosis apparatus (Millipore, Bedford, MA). DMMP [2.92% (w/w)] was dissolved in neat H_2O. Lysozyme (1.0 mM) was dissolved in phosphate-buffered saline (PBS; Na_2HPO_4/NaH_2PO_4 buffer with 10 mM total phosphate, pH = 6.33; NaCl added to osmolality 289 ± 2 mmol kg^{-1}). To prevent microbial growth, NaN_3 was added to the lysozyme solution [3 drops of 0.1% (w/v) NaN_3 per 50 mL], and to eliminate cellular material, the solution was filtered sequentially through 0.45 μm and 0.2 μm cellulose acetate filters. The solutions were stored at 2 ^oC and used one day after preparation.

NMR setup and measurements

All measurements were on a Bruker DRX-400 NMR spectrometer equipped with a 1000 G cm^{-1} *z*-only actively shielded diffusion probe [18,19]. Sample temperature was calibrated using a capillary containing ethylene glycol. The DMMP/water sample was studied in a 5-mm Shigemi (Allison Park, PA) tube matching the magnetic susceptibility of D_2O. The lysozyme/water sample was studied in a cylindrical 8-mm outer-diameter Wilmad (Buena, NJ) microcell inserted into a 10 mm tube containing CCl_4 for susceptibility matching. In either case, the sample length was constrained to 8-9 mm in order to contain the sample within the probe's constant-gradient region [18]. No special precautions were taken against possible radiation damping, because the diffusion coefficient of water was not used in the interpretation of results. Diffusion measurements were made using a number of different pulse sequences to enable a comparison of results; their general setup has been described before [18]. Trapezoidal gradient pulses with ramp times τ = 0.1 ms and effective durations δ = 1 ms (all ^1H measurements) or 2 ms (^{31}P measurements) were used. Stejskal–Tanner plots were processed according to Eq. (9). Soft-π pulses in both CONVEX and PGSE-Watergate experiments were selective Gaussian pulses with 2-ms duration. Their power was optimized for maximum efficiency of water suppression (or, in the case of the PGSE-Watergate, for maximum solute signal) separately for each experiment and each Δ used. Scan repetition times were 5 times the longest T_1 value.

Primary processing of NMR data and integration of spectral peaks was performed in the Bruker XWIN-NMR software. The diffusion coefficients *D* were determined from linearized fitting in *Mathematica*, in Stejskal-Tanner coordinates assuming trapezoidal gradient pulses [16,18,19]. The standard deviations of *D* were obtained from the linear regression.

Results

A series of comparative measurements of the diffusion coefficients of 2.92% (w/w) dimethyl methylphosphonate (DMMP) in water and 1.0 mM lysozyme in PBS were used to test the proposed CONVEX experiment. In all, five types of measurements were used (although not all of them were carried out on each sample): (1) basic PGSE [20]; (2) convection-compensated PGSE without water suppression [11]; (3) PGSE-Watergate [1]; (4) CONVEX with uncentered hard-π pulses; and (5) CONVEX with centered hard-π pulses. In the centered CONVEX experiment, the hard-π pulses were centered within the bracketed intervals shown in Fig. 2A. In the uncentered version, the soft-π pulse was placed 1 ms after the sensitizing gradient pulse, and the hard-π pulse was placed immediately before the refocusing gradient pulse. In view of the short diffusion intervals used, stimulated-echo measurements were deemed unnecessary.

Three groups of measurements were carried out; each group consisted of the same sample measured by different methods under identical conditions. The D of DMMP in water at 23 ^{o}C was determined from ^{31}P and ^{1}H measurements. Four ^{31}P measurements: PGSE with $\Delta = 10$ ms and $\Delta = 26$ ms and convection-compensated PGSE with $\Delta = 5$ ms and $\Delta = 13$ ms, and four ^{1}H measurements: PGSE with $\Delta = 4.88$ ms and convection-compensated PGSE, uncentered and centered CONVEX, each with $\Delta = 4.878$ ms, were made in this group. The CONVEX measurements were made with $C = 0.7143 \approx 5/7$. For each measurement, the diffusion coefficients were determined separately from baseline-corrected and baseline-uncorrected spectra. The results are given in Tables 1 and 2. Representative Stejskal–Tanner plots showing the determination of the linear attenuation range of the signal are presented in Fig. 3. The purpose of this group of measurements was to verify that the diffusion and water-suppression sides of the CONVEX experiment worked correctly. With respect to diffusion attenuation, the aim was to establish that it was consistent with the theoretically predicted Eq. (9), as well as with the diffusion coefficients measured from ^{31}P and non-water-suppressed ^{1}H spectra. With respect to water suppression, the aim was to verify that CONVEX produced high-quality spectra with no phase or baseline distortions and good water suppression efficiency, and provided an enhancement of the linear range of signal attenuation compared to ^{31}P and non-water-suppressed ^{1}H spectra. Another goal was to evaluate the sensitivity of the resulting diffusion coefficients to baseline correction of the spectra.

The *D* of DMMP in water at 47.4 ± 0.5 ^{o}C was also determined from ^{31}P and ^{1}H measurements. Four ^{31}P measurements: PGSE with Δ = 10 ms and Δ = 26 ms and convection-compensated PGSE with Δ = 5 ms and Δ = 13 ms, and seven ^{1}H measurements: PGSE with Δ = 5 ms and 13 ms, convection-compensated PGSE with Δ = 5 ms and 13 ms, uncentered CONVEX with Δ = 5 ms, and centered CONVEX with Δ = 5 ms and 13 ms (*C* = 0.7143), were made. Only baseline-corrected spectra were used in this group for the determination of the diffusion coefficients. The results are given in Tables 3 and 4. The purpose of this group of measurements was to test the functioning of convection compensation in CONVEX, and to evaluate the effect of convection on the quality of the resulting spectra.

The last group involved the measurement of *D* of lysozyme in PBS at 38.0 ± 0.5 ^{o}C using convection-compensated PGSE, PGSE-Watergate, and centered CONVEX (*C* = 0.7143), each from ^{1}H spectra with Δ = 5 ms. The diffusion coefficient of lysozyme was measured independently from four groups of peaks in convection-compensated PGSE and CONVEX, and from a single group of peaks in PGSE-Watergate. Only baseline-corrected spectra were used in this group; the results are given in Table 5. The sample used for these measurements had a smaller aspect ratio than the DMMP sample, and therefore the shimming line width was greater (~10 Hz vs ~3 Hz, respectively). The purpose of this group of measurements was therefore to test the behavior of the CONVEX experiment with a different sample geometry and a significantly lower diffusion coefficient (approximately an order of magnitude less than that of a typical small molecule in water).

Discussion

Room-temperature measurements. Diffusion measurements in water at 23 ^{o}C (i.e., near room temperature) normally do not require convection compensation because convection is negligible under these conditions. Therefore, measurements of DMMP in water at 23 ^{o}C serve as "ideal-conditions" tests of the diffusion experiments. From the six measurements done without water suppression, the average D of DMMP was $(8.25 \pm 0.16) \times 10^{-10}$ m^2 s^{-1} from baseline-corrected measurements and $(8.3 \pm 0.4) \times 10^{-10}$ m^2 s^{-1} from baseline-uncorrected measurements. These results were consistent with the diffusion coefficients from CONVEX measurements: the average baseline-corrected D from uncentered CONVEX was $(8.29 \pm 0.06) \times 10^{-10}$ m^2 s^{-1}, and that from the centered version was $(8.16 \pm 0.05) \times 10^{-10}$ m^2 s^{-1}. Therefore, diffusion attenuation in CONVEX experiments was consistent with that predicted by Eqs. (8) and (9).

Figure 4 shows representative baseline-corrected spectra from CONVEX (Fig. 4B, C) and non-water suppressed double-echo PGSE (Fig. 4A) measurements, with the vertical scale chosen to emphasize residual baseline imperfections. Inspection of this Figure reveals that CONVEX provided a remarkable improvement of spectral baseline compared to non-water suppressed convection-compensated measurements. Without water suppression, baseline distortions survived polynomial correction at least up to g = 1.5 T m^{-1}, which corresponded to a 3- to 4-fold diffusion attenuation of DMMP. These distortions were caused either by minor phase distortions of the large water signal (dispersive baseline), or its imperfect digitization (rolling baseline), and could not be remedied by non-interactive baseline-correction methods. In spectra with a significantly attenuated water signal the severity of "uncorrectable" baseline distortions decreased; large-g spectra tended to suffer only distortions amenable to first-order polynomial correction. A similar situation was observed in PGSE measurements without convection compensation.

In CONVEX measurements, the water peak was attenuated to below the intensity of DMMP peaks within $g_1 \sim 0.5$ T m^{-1}. Because no large water peak was present outside this range of g, only the first few low-g spectra suffered from dispersive or rolling baseline. Medium- and large-g spectra from uncentered-CONVEX measurements showed small quadratic distortions; in centered-CONVEX spectra, small linear distortions were present. Both were easily corrected using a non-interactive polynomial correction of the appropriate order.

Even more encouraging was the fact, seen from Table 2, that *D* estimates from either version of CONVEX were insensitive to baseline correction. The deviations of the integrals of DMMP peaks were very small and random, and the application of baseline correction influenced the resulting values of *D* by less than the precision of the measurement. We attribute this outcome to the absence of the baseline distortions associated with a large water signal.

Because of the dramatically improved baseline and the consequentially improved accuracy of peak integration, CONVEX provided Stejskal–Tanner plots with larger linear regions than PGSE measurements without water suppression. Although more low-*g* CONVEX points were unusable than in conventional PGSE measurements, the linear region extended much farther into large-*g* values in CONVEX than in conventional measurements. Each of the non-water suppressed measurements shown in Table 2 provided a region of linear Stejskal–Tanner attenuation of 1.5, which corresponded to ~30-fold attenuation of DMMP peaks. On the other hand, the linear region was >2 in uncentered-CONVEX and 2.6 in centered-CONVEX measurements. This corresponded to the attenuation of DMMP signals by >100 and ~400, respectively, which is an excellent performance for a solute of low-concentration in a non-deuterated solvent.

High-temperature measurements. Although the CONVEX experiment provided excellent results under "ideal" conditions, its performance must ultimately be evaluated in the presence of thermal convection. This test was provided by DMMP/water measurements at 47.4 ^{o}C, whose results are shown in Tables 3 and 4. The diffusion coefficient of DMMP obtained from non-convection-compensated ^{1}H PGSE measurements at Δ = 13 ms [$(1.59 \pm 0.01) \times 10^{-9}$ m^2 s^{-1}] was ~9% larger than at Δ = 5 ms [$(1.46 \pm 0.01) \times 10^{-9}$ m^2 s^{-1}]. A similar trend was observed in ^{31}P measurements. Therefore, convection under these conditions was severe enough to have affected the measured *D* value. On the other hand, convection-compensated PGSE measurements produced Δ- and γ-independent diffusion coefficients: ^{31}P measurements at Δ = 5 and 13 ms and ^{1}H measurements at Δ = 5 ms were in excellent agreement with each other [$D = (1.39 \pm 0.02) \times 10^{-9}$ m^2 s^{-1}]. The results of conventional convection-compensated ^{1}H PGSE measurement at Δ = 13 ms were unusable due to overwhelming spectral peak breakup and the resulting deterioration of the accuracy of peak integration; a representative example is shown in Figs. 5A and 5B.

The diffusion coefficient obtained from CONVEX experiments with Δ_1 = 5 ms and 13 ms was $(1.37 \pm 0.03) \times 10^{-9}$ m^2 s^{-1}, which is in agreement with the results from convection-

compensating measurements without water suppression. Figures 5C and 5D show representative medium-*g* CONVEX spectra. Their quality at the long Δ value compared favorably to that from the non-water suppressed measurement. Baseline distortions followed the same trends as seen at 23 ^{o}C. Spectra from convection-compensating measurements without water suppression exhibited baseline roll and dispersion, especially at low *g* values. In CONVEX spectra, serious distortions were localized to the first few low-*g* spectra with incomplete suppression of the water peak (which were discarded). Although the noise level in CONVEX spectra was ~8× greater than in non-water suppressed double PGSE spectra (see Fig. 5), baseline distortions in the former were considerably smaller and easily remedied by non-interactive polynomial correction. Of course, in the conventional double-PGSE measurement with Δ = 13 ms severe spectral peak breakup presented a far more serious problem than baseline distortions.

As was the case at 23 ^{o}C, Stejskal–Tanner plots obtained from CONVEX measurements at 47.4 ^{o}C were linear over a greater signal attenuation range than non-water suppressed experiments. The linear range of CONVEX measurements averaged 2.3 decades. The range of linearity in non-convection compensating PGSE measurements (2.2) was formally as good as in CONVEX; however, this was hardly useful, because non-convection-compensating PGSE failed to yield the "correct" diffusion coefficient (see Tables 3 and 4). In conventional convection-compensating PGSE measurement with Δ = 5 ms, which did yield the correct *D*, the linear Stejskal–Tanner range (1.8) was half an order of magnitude smaller than in the respective CONVEX measurement (2.3).

Similar trends were observed for diffusion measurements of lysozyme in PBS (pH 6.33), carried out at 38.0 ^{o}C in a diffusion microcell with an aspect ratio close to 1. The results of these measurements are listed in Table 5. PGSE-Watergate measurement provided an overestimated apparent diffusion coefficient, presumably due to convection. The results obtained from convection-compensating PGSE without water suppression, and from CONVEX measurements, were consistent with each other [$(1.47 \pm 0.1) \times 10^{-10}$ and $(1.47 \pm 0.05) \times 10^{-10}$ $m^2\ s^{-1}$, respectively], as well as with data from the literature (experimentally measured *D* in a 1.5 mM lysozyme saline solution at pH 6 and 35 ^{o}C was 1.48×10^{-10} $m^2\ s^{-1}$; theoretically predicted monomer *D* under the same conditions was 1.5×10^{-10} $m^2\ s^{-1}$) [21]. Severe baseline distortions in CONVEX spectra were localized to a narrower range of *g* values than in the absence of water suppression. The linear range in CONVEX Stejskal–Tanner plots was almost an order of

magnitude greater than in convection-compensating PGSE without water suppression (1.9 and 1.1, respectively).

General remarks. Many of the general features of PGSE-based experiments, extensively discussed in the literature, are common to CONVEX. As is always the case with transverse magnetization storage [7], scalar couplings modulate the amplitude of the CONVEX signal with respect to the diffusion interval Δ. CONVEX does not compensate for non-linearity of field gradients; therefore, one should ensure that appropriate processing methods are used if the sample extends outside the constant-gradient region [22]. Finally, using very long Δ may adversely affect the quality of solvent suppression [5]; however, Δ-specific calibration of the power of the soft-π pulses offsets this effect. A detailed discussion of these issues is found in the literature.

Conclusions

Double-echo PGSE convection compensation and double excitation-sculpting solvent suppression can be combined in a single pulse sequence when used with unequal diffusion intervals, $\Delta_1 \neq \Delta_2$, and gradient pulse strengths $g_1 : g_2 = \Delta_2 : \Delta_1$. The resulting experiment (CONVEX) can be used for measuring solute diffusion coefficients in non-deuterated solvents at high temperatures. Its robustness is further enhanced by centering the hard-π pulses to refocus chemical shifts and local field inhomogeneities exactly at the beginning of acquisition. In test measurements, CONVEX yielded superb-quality spectra with no phase distortions and no more than minor, non-interactively corrected baseline distortions. Efficient solvent suppression required that the gradient pulse strengths were above a certain threshold, and the first few low-*q* spectra typically were discarded. However, CONVEX provided an overall enhancement of the linear signal attenuation range due to the improved spectral baseline. CONVEX measurements provided correct values of the diffusion coefficients both in the presence and in the absence of convection, and the resulting *D* values were insensitive to baseline correction. In the presence of strong convection, peak breakup at long Δ values was considerably less serious in CONVEX than in the conventional convection-compensating PGSE, making CONVEX usable over a greater range of Δ values. We expect that the new experiment will be useful for the characterization of proteins; biological or cellular systems; or for the monitoring of technological processes.

Acknowledgements. This work was supported by an ARC-SPIRT grant to PWK and KIM. We thank Dr. Tom Eykyn and Prof. Bill Price for helpful discussions, Mr. Bill Lowe for technical assistance, and Drs. Bill Bubb and Bob Chapman for NMR spectroscopic assistance.

References

[1] W.S. Price, F. Elwinger, C. Vigouroux, P. Stilbs, PGSE-WATERGATE, a new tool for NMR diffusion-based studies of ligand-macromolecule binding, Magn. Reson. Chem. 40 (2002) 391-395.

[2] J. Cavanagh, W.J. Fairbrother, A.G. Palmer, N.J. Skelton, Protein NMR Spectroscopy: Principles and Practice, Academic Press, San Diego, 1996.

[3] P.W. Kuchel, C.J. Durrant, B.E. Chapman, P.S. Jarrett, D.G. Regan, Evidence of red cell alignment in the magnetic field of an NMR spectrometer based on the diffusion tensor of water, J. Magn. Reson. 145 (2000) 291-301.

[4] A.J. Weekley, P. Bruins, M. Sisto, M.P. Augustine, Using NMR to study full intact wine bottles, J. Magn. Reson. 161 (2003) 91-98.

[5] T.L. Hwang, A.J. Shaka, Water suppression that works - excitation sculpting using arbitrary wave-forms and pulsed-field gradients, J. Magn. Reson. A 112 (1995) 275-279.

[6] M. Piotto, V. Saudek, V. Sklenar, Gradient-tailored excitation for single-quantum NMR spectroscopy of aqueous solutions, J. Biomol. NMR 2 (1992) 661-665.

[7] C.S. Johnson, Diffusion ordered nuclear magnetic resonance spectroscopy: principles and applications, Prog. Nucl. Magn. Reson. Spectrosc. 34 (1999) 203-256.

[8] J.B. Cain, K. Zhang, D.E. Betts, J.M. DeSimone, C.S. Johnson, Diffusion of block copolymers in liquid CO_2: evidence of self-assembly from pulsed field gradient NMR, J. Am. Chem. Soc. 120 (1998) 9390-9391.

[9] W.J. Goux, L.A. Verkruyse, S.J. Salter, The impact of Rayleigh-Bénard convection on NMR pulsed-field-gradient diffusion measurements, J. Magn. Reson. 88 (1990) 609-614.

[10] A. Jerschow, N. Müller, Suppression of convection artifacts in stimulated-echo diffusion experiments. Double-stimulated-echo experiments, J. Magn. Reson. 125 (1997) 372-375.

[11] G.H. Sørland, J.G. Seland, J. Krane, H.W. Anthonsen, Improved convection compensating pulsed field gradient spin-echo and stimulated-echo methods, J. Magn. Reson. 142 (2000) 323-325.

[12] A. Jerschow, Thermal convection currents in NMR: flow profiles and implications for coherence pathway selection, J. Magn. Reson. 145 (2000) 125-131.

[13] A. Jerschow, N. Müller, Convection compensation in gradient enhanced nuclear magnetic resonance spectroscopy, J. Magn. Reson. 132 (1998) 13-18.

[14] Y. Xia, P.T. Callaghan, Imaging the velocity profiles in tubeless siphon flow by NMR microscopy, J. Magn. Reson. 164 (2003) 365-368.

[15] C.S. Johnson, Diffusion measurements by magnetic field gradient methods, in: D.M. Grant, R.K. Harris (Eds.), Encyclopedia of Nuclear Magnetic Resonance, Wiley, New York, 1996, pp. 1626-1644.

[16] K.I. Momot, P.W. Kuchel, Pulsed field gradient nuclear magnetic resonance as a tool for studying drug delivery systems, Concepts Magn. Reson. 19A (2003) 51-64.

[17] A. Jerschow, Unwanted signal leakage in excitation sculpting with single axis gradients, J. Magn. Reson. 137 (1999) 206-214.

[18] K.I. Momot, P.W. Kuchel, B.E. Chapman, P. Deo, D. Whittaker, NMR study of the association of propofol with nonionic surfactants, Langmuir 19 (2003) 2088-2095.

[19] K.I. Momot, P.W. Kuchel, D. Whittaker, Enhancement of Na^+ diffusion in a bicontinuous cubic phase by the ionophore monensin, Langmuir 20 (2004) in press.

[20] E.O. Stejskal, J.E. Tanner, Spin diffusion measurements: spin echoes in the presence of a time-dependent field gradient, J. Chem. Phys. 42 (1965) 288-292.

[21] W.S. Price, F. Tsuchiya, Y. Arata, Lysozyme aggregation and solution properties studied using PGSE NMR diffusion measurements, J. Am. Chem. Soc. 121 (1999) 11503-11512.

[22] P. Damberg, J. Jarvet, A. Gräslund, Accurate measurement of translational diffusion coefficients: a practical method to account for nonlinear gradients, J. Magn. Reson. 148 (2001) 343-348.

Figure Captions

Figure 1. Pulse sequences for: **(A)** double-echo convection-compensating PGSE [11]; **(B)** double-echo excitation-sculpting water suppression with single-axis gradient pulses [5]. In both experiments, the hard π-pulses are centered within the respective bracketed intervals, and all pulsed gradients are applied along the *z*-axis. In **(A)**, the two pairs of gradients have the same amplitude; convection compensation is achieved by inverting the sign of **q** [see Eq. (2)] during the second Δ. In **(B)**, the amplitudes of the two pairs of gradients are mutually prime if they are applied along the same axis; this enhances water-suppression efficiency by reducing "signal leakage" [17]. The power of the soft π-pulses is optimized for maximum water-suppression efficiency.

Figure 2. (A) Pulse sequence for the proposed CONVEX experiment. The experiment combines convection-compensating PGSE [11] with double-echo excitation-sculpting water suppression [5]. The amplitudes of the two pairs of gradient pulses, g_1 and g_2, are mutually prime to ensure efficient water suppression. The convection-compensation criterion, Eq. (4), is satisfied by setting $\Delta_1 : \Delta_2 = g_2 : g_1$, in order to make the time integrals of **q** in Δ_1 and Δ_2 equal by absolute value. **(B)** The evolution of **q**, as defined in Eq. (2), during the CONVEX pulse sequence. The areas of the two shaded trapezoids are equal.

Figure 3. Representative Stejskal–Tanner plots showing how the linear range of signal attenuation was determined. The PGSEcc plot (solid triangles) was shifted vertically in order to resolve it from the CONVEX plot (empty circles). The first few points of the PGSEcc plot were discarded because of baseline distortions.

Figure 4. Representative baseline-corrected spectra of DMMP in water at 23 ^{o}C from: **(A)** convection-compensated PGSE with Δ = 4.878 ms; **(B)** uncentered CONVEX; and **(C)** centered CONVEX experiments with Δ_1 = 4.878 ms and C = 0.7143. The respective gradient pulse amplitudes are marked next to the spectra. Relative diffusion attenuation is approximately the same between the three groups. Each spectrum was the result of four transients. Because water-suppressed and non-water suppressed spectra were recorded with different values of the receiver gain, the vertical scale was normalized separately within each group by the amplitude of the O–CH_3 doublet (3.7 ppm) at $g \rightarrow 0$. The normalized vertical scale is the same for all spectra, except the first spectrum in **(A)**, which was plotted with a smaller scale to enable a full view of the baseline.

Figure 5. Effect of strong convection on the line shapes in double-echo spectra. Water signal (4.8 ppm) and O–CH_3 DMMP doublet (3.9 ppm) in representative baseline-corrected spectra of DMMP in water at 47.4 ± 0.5 ^{o}C: **(A)** convection-compensated PGSE with Δ = 5 ms; **(B)** convection-compensated PGSE with Δ = 13 ms; **(C)** centered CONVEX with Δ_1 = 5 ms and C = 0.7143; and **(D)** centered CONVEX with Δ_1 = 13 ms and the same C. Relative diffusion attenuation was approximately the same in each of the four spectra (12–15-fold). Each spectrum was the result of four transients. The vertical scale of each spectrum was normalized separately by the amplitude of the DMMP doublet at $g \rightarrow 0$.

Tables

Table 1. Diffusion coefficients of DMMP in water at 23 °C obtained from ^{31}P PGSE measurements.

Pulse sequence [a]	Δ (ms)	Baseline correction order [b]	D (m^2 s^{-1}) × 10^{10}	Linear range [c]
PGSE	10	1	8.07 ± 0.1	1.0
		–	8.01 ± 0.1	1.4
PGSE	26	1	8.04 ± 0.1	1.4
		–	8.18 ± 0.1	1.5
PGSEcc	5	1	8.17 ± 0.1	1.3
		–	8.11 ± 0.1	1.0
PGSEcc	13	1	8.43 ± 0.1	1.5
		–	8.63 ± 0.1	1.5

a) PGSE, basic PFG spin-echo measurements [20]; PGSEcc, double-echo convection-compensating PGSE without water suppression [11].

b) 1, first-order polynomial correction; –, baseline-uncorrected spectra.

c) "Linear range" is the range of signal attenuation (in decades) over which the respective Stejskal–Tanner plot was linear; refer to Fig. 3 for an illustration.

Table 2. Diffusion coefficients of DMMP in water at 23 ^{o}C obtained from ^{1}H PFG measurements.

Pulse sequence	Δ (ms)	Baseline correction order	D (m^2 s^{-1}) × 10^{10} [a]	Linear range[b]	Baseline distortions
PGSE	4.88	1	8.28 ± 0.1 8.13 ± 0.1	1.5 1.5	Serious at $g \leq$ 2.9 T m^{-1}
		–	8.60 ± 0.1 8.85 ± 0.1	1.2 1.2	
PGSEcc	4.878	1	8.44 ± 0.1 8.47 ± 0.1	1.5 1.5	Serious at $g \leq$ 1.8 T m^{-1}
		–	8.16 ± 0.1 7.68 ± 0.1	1.5 1.2	
CONVEX (uncentered)	4.878	2	8.35 ± 0.1 8.23 ± 0.1	2.1 2.4	Serious at $g_1 \leq$ 0.5 T m^{-1}; minor quadratic thereafter
		–	8.15 ± 0.1 8.28 ± 0.1	1.8 1.6	
CONVEX (centered)	4.878	1	8.11 ± 0.1 8.20 ± 0.1	2.6 2.6	Serious at $g_1 \leq$ 0.5 T m^{-1}; minor linear thereafter
		–	8.15 ± 0.1 8.25 ± 0.1	2.6 2.6	

[a] The two values in each measurement refer to the two DMMP doublets, P–CH_3 (1.6 ppm) and O–CH_3 (3.7 ppm), respectively.

[b] Refer to Fig. 3. In CONVEX, the linear range took into account the discarded initial points, which were normally unusable because of the incompletely suppressed water peak.

Table 3. Diffusion coefficients of DMMP in water at 47.4 ± 0.5 ^{o}C obtained from baseline-corrected (first-order polynomial) ^{31}P PGSE measurements.

Pulse sequence	Δ (ms)	D (m^2 s^{-1}) × 10^9	Linear range
PGSE	10	1.60 ± 0.02	1.8
PGSE	26	1.79 ± 0.02	1.7
PGSEcc	5	1.37 ± 0.02	1.6
PGSEcc	13	1.41 ± 0.05	1.0

Table 4. Diffusion coefficients of DMMP in water at 47.4 ± 0.5 °C obtained from baseline-corrected ^{1}H PFG measurements.

Pulse sequence	Δ (ms)	D (m^2 s^{-1}) × 10^9 [a]	Linear range	Baseline corr. order	Baseline distortions
PGSE	5	1.46 ± 0.01 1.46 ± 0.01	2.0 2.1	1	Minor roll and correctable offset
PGSE	13	1.59 ± 0.01 1.59 ± 0.01	2.3 2.3	1	Correctable offset
PGSEcc	5	1.39 ± 0.02 1.40 ± 0.02	1.8 1.8	1	Roll and correctable offset
PGSEcc	13	unusable (severe line breakup)	< 1	–	Minor roll
CONVEX (uncentered)	5	1.36 ± 0.01 1.39 ± 0.01	3.1 2.4	2	Serious at $g_1 \leq$ 0.5 T m^{-1}; minor quadratic thereafter
CONVEX (centered)	5	1.32 ± 0.01 1.37 ± 0.01	2.1 2.4	2	Serious at $g_1 \leq$ 0.2 T m^{-1}; practically flat at $g_1 \geq$ 0.9 T m^{-1}
CONVEX (centered)	13	1.36 ± 0.05 1.41 ± 0.05	1.8 2.0	1	Moderate line breakup at $g_1 \leq$ 0.6 T m^{-1}; flat thereafter

[a] The two values in each measurement refer to the two DMMP doublets.

Table 5. Diffusion coefficients of lysozyme in water at 38.0 ± 0.5 °C obtained from baseline-corrected ^{1}H PFG measurements.

Pulse sequence	Δ (ms)	D (m^2 s^{-1}) × 10^{10} [a]	Linear range	Baseline corr. order	Baseline
PGSEcc	5	1.61 ± 0.02 1.45 ± 0.03 1.40 ± 0.03 1.41 ± 0.02	0.9 1.3 1.0 1.3	1	Serious roll at $g \leq$ 1.4 T m^{-1}; correctable offset thereafter
PGSE-WATERGATE	5	1.66 ± 0.05	0.5	1	Uncorrectable at $g_1 \leq$ 0.2 T m^{-1}; flat thereafter
CONVEX (centered)	5	1.43 ± 0.01 1.52 ± 0.01 1.43 ± 0.01 1.49 ± 0.01	1.6 2.0 2.1 1.8	1	Uncorrectable at $g \leq$ 0.7 T m^{-1}; correctable offset thereafter

[a] Different D values in the PGSEcc and CONVEX measurements refer to different groups of lysozyme protons (9.36–7.95, 7.92–6.94, 3.38–2.55, and 1.86–0.89 ppm; water peak was assigned to 4.8 ppm). A single group (1.86–0.89 ppm) was used in the PGSE-Watergate measurement. The PGSE-Watergate D was obtained from the slow component of the biexponential Stejskal–Tanner plot.

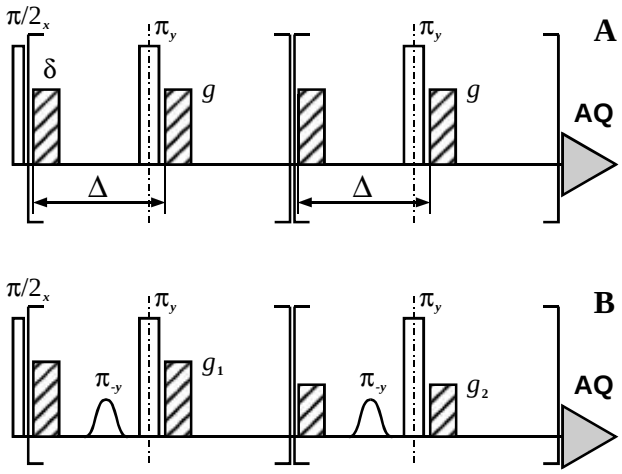

Figure 1, Momot & Kuchel,
Convection Compensation with Water Suppression

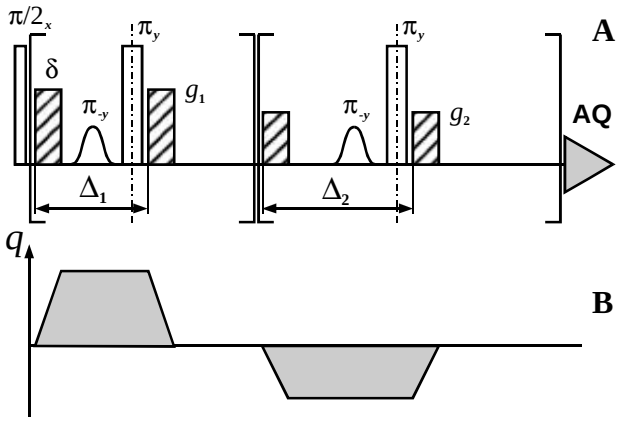

Figure 2, Momot & Kuchel,
Convection Compensation with Water Suppression

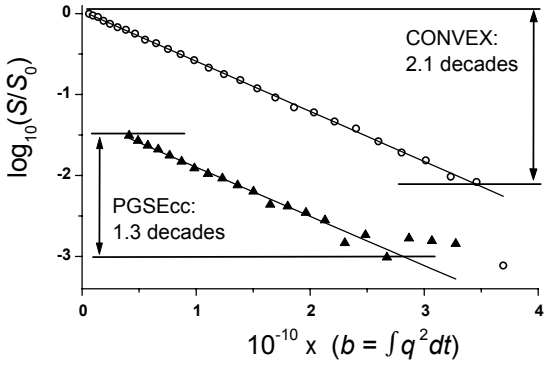

Figure 3, Momot & Kuchel,
Convection Compensation with Water Suppression

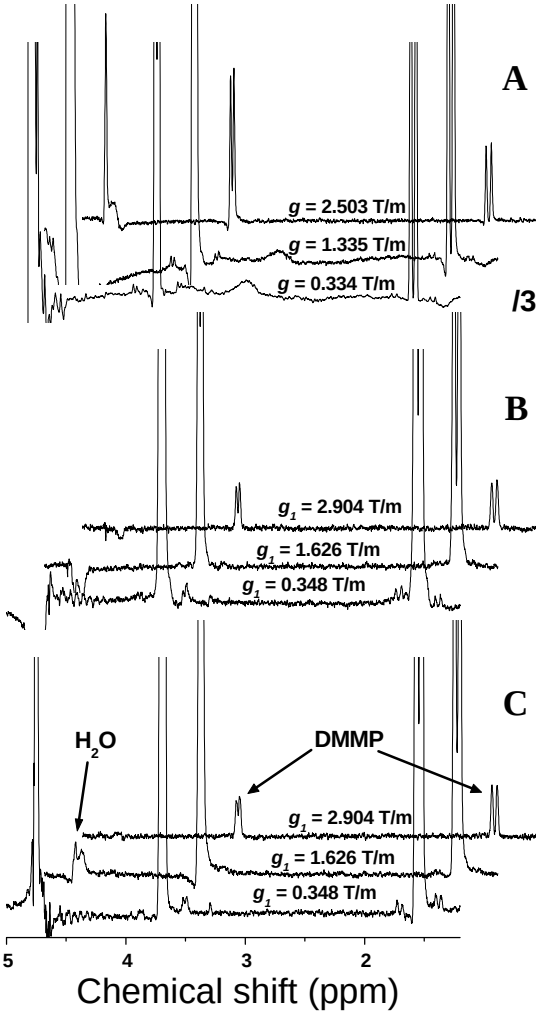

Figure 4, Momot & Kuchel,
Convection Compensation with Water Suppression

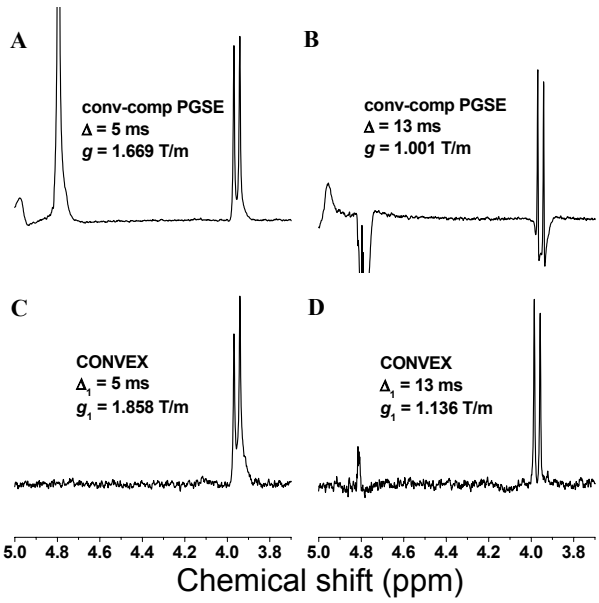

Figure 5, Momot & Kuchel,
Convection Compensation with Water Suppression